Electrochimica Acta 98 (2013) 199–207

Contents lists available at SciVerse ScienceDirect

Electrochimica Acta

journal homepage: www.elsevier.com/locate/electacta

Synthesis, characterization and influence of poly(brilliant green) on the performance of different electrode architectures based on carbon nanotubes and poly(3,4-ethylenedioxythiophene)

Valentina Pifferi[a,b,1], Madalina M. Barsan[a], M. Emilia Ghica[a,1], Luigi Falciola[b,1], Christopher M.A. Brett[b,*,1]

[a] Departamento de Química, Faculdade de Ciências e Tecnologia, Universidade de Coimbra, 3004-535 Coimbra, Portugal
[b] Dipartimento di Chimica, Università degli Studi di Milano, Via Golgi 19, 20133 Milano, Italy

ARTICLE INFO

Article history:
Received 8 January 2013
Received in revised form 8 March 2013
Accepted 9 March 2013
Available online xxx

Keywords:
Brilliant green
Carbon film
Carbon nanotubes
Poly(3,4-ethylenedioxythiophene)
Hydrogen peroxide

ABSTRACT

Brilliant green (BG), which belongs to the triphenylmethane family, has been electrochemically polymerised by cyclic voltammetry on bare carbon film electrodes (CFE) and for the first time on carbon nanotubes (CNTs) and poly(3,4-ethylenedioxythiophene) (PEDOT) modified CFE. The modified electrodes have been characterized by cyclic voltammetry (CV) and electrochemical impedance spectroscopy (EIS) in order to establish the position importance and the individual role of each component (CNT, PEDOT and PBG) in the overall electrode performance. The analytical performances of different electrode architectures towards hydrogen peroxide detection allowed the choice of the best electrode configuration for further application of the newly developed electrodes for sensor and biosensor construction.

1. Introduction

In recent years, conducting polymers have been used to fabricate fuel cells, electrochemical capacitors, batteries, memory devices, electrochromic devices, electrochemical actuators, field emission devices, superhydrophobic coatings and (bio)sensors. In particular, their use in the field of electrochemical sensors seems to be very promising, since they allow the enhancement of speed, sensitivity and versatility [1,2]. Conducting polymers have a conjugated chain structure, which presents an extended π-bond system, leading to the formation of broad valence and conduction bands. They can be generated by electropolymerisation which permits a good control of the polymer structure [3,4] and, due to their high conductivity, well-defined and versatile structure, simple synthesis and high resistance, they have increasing applications.

Among all the types of conducting polymers, electroactive polymers seem to have the best qualities for sensor construction [5–7]. Besides the high conductivity, they can act as electron donors/acceptors, exhibiting electrocatalytic effects and the possibility of redox-mediation. Polyphenazines are a class of electroactive polymers introduced successfully in the 1990s to build new and very sensitive modified electrodes [8]. These types of sensor can detect a wide range of organic and inorganic compounds, such as NADH, nitrites, cysteine, haemoglobin, carboxylic acids, vitamin B_6 and epinephrine [9], using different techniques, such as cyclic voltammetry, pulsed methods and amperometry, also being used for the construction of biosensors for alcohol, acetaldehyde, glucose, glycerol and pyruvate [9,10].

Similar to these azine dyes, triphenylmethanes are dye compounds, used in textile dying and paper printing, and as antiseptic, antifungal and antimicrobial agents in aquaculture and in the food industry [11,12]. The fact that they have an open, ionized structure is promising for fast charge transfer and for catalytic ability in ionic transport, which is very useful in the field of sensors. In recent years, malachite green (MG), a member of this class of triphenylmethane dyes, was successfully electropolymerised on glassy carbon electrodes [13] and tested for the detection of dopamine [14], NADH and ascorbic acid [15]. A very recent report is the only one on triphenylmethane electropolymerisation and concerns brilliant green (BG) [16]. BG belongs to the triphenylmethane family, the same as MG, and has been used as a biological stain and bacteriostatic agent in culture media and veterinary medicine [17,18]; however, it has never been used previously in the field of sensors, except for ascorbate in Ref. [16].

---

[*] Corresponding author. Tel.: +351 239854470; fax: +351 239827703.
E-mail address: cbrett@ci.uc.pt (C.M.A. Brett).

[1] ISE member.

0013-4686/$ – see front matter © 2013 Elsevier Ltd. All rights reserved.
http://dx.doi.org/10.1016/j.electacta.2013.03.048

In this work, the electropolymerisation of BG on carbon film electrodes together with deposition of CNTs and PEDOT is reported for the first time. In one configuration 3,4-ethylenedioxythiophene (EDOT) was polymerised together with brilliant green. The PEDOT polymer belongs to the class of conjugated polymers, and was chosen here due to its unique properties, such as high conductivity, good stability under ambient conditions, moderate band gap, low oxidation potential and transparency [19,20], which permits its application in the field of supercapacitors [21] and more recently in electrochemistry. PEDOT can be used alone [22,23], in combination with electroactive polymers to obtain composites with improved properties [24,25], or in combination with nanoparticles [26,27], to improve the performance of different types of sensors. The electrode architecture developed in this work contained, beside PEDOT, carbon nanotubes (CNTs) [28,29], since the association of CNTs and conducting polymers, initially used for energy conversion and storage purposes [30], is very attractive, due to the combination of the complementary properties of polymers and CNTs [31]. In the recent literature, very sensitive electrodes based on CNTs and conducting polymers were reported for the detection of hydrogen peroxide [32], glucose [33,34] and organochlorine pesticides [35]. However, only one example of electrodes with CNTs in combination with polytriphenylmethanes was found, poly(malachite green) for the detection of catechol and quinol [36].

Thus, new electrodes based on poly(brilliant green) (PBG) as electroactive polymer in combination with PEDOT and CNTs were prepared and characterized by cyclic voltammetry and electrochemical impedance spectroscopy. The electrode platforms were tested for the detection of hydrogen peroxide in order to investigate the influence of different configurations and components on the performance, with the view of developing new sensors and biosensors based on these architectures.

2. Experimental

2.1. Reagents and solutions

All reagents were of analytical grade and used as received.

The solution for the polymerisation of EDOT (Aldrich) contained 0.01 M of monomer dissolved in 0.1 M 4-styrenesulphonic acid sodium salt hydrate (NaSS) (Aldrich). The electrolyte for the electropolymerisation of BG (Fluka) was 0.1 M McIlvaine buffer pH 4.0 (Aldrich).

CNTs (NanoLab, USA) were functionalized in 5 M nitric acid 65% and dispersed in a solution 1% chitosan (low molecular weight, degree of deacetylation 80%), which was prepared in 1% glacial acetic acid, both from Aldrich.

The electrolyte used for the electrochemical characterization of all the electrodes was 0.1 M potassium chloride (KCl) from Panreac.

Phosphate buffer saline (PBS) pH 7.0, containing 0.1 M NaPB ($Na_2HPO_4 + NaH_2PO_4$ from Riedel-de-Haën) and 0.05 M NaCl (Aldrich) were used for the detection of H_2O_2 (Panreac, Spain).

Millipore Milli-Q nanopure water (resistivity $\geq 18\,M\Omega\,cm^{-1}$) was used for the preparation of all solutions.

2.2. Instrumentation

An electrochemical cell with a modified carbon film electrode (CFE, geometric area $0.2\,cm^2$, resistance $2\,\Omega$, film thickness $15\,\mu m$) as working electrode, a Pt wire as counter electrode and a saturated calomel electrode (SCE) as reference electrode were used in all the experiments. The carbon film electrodes are made from carbon film resistors with a carbon film formed by pyrolysis on a ceramic cylindrical substrate and with two tight-fitting metal caps linked to wires as external contact. The procedure to make electrodes consists in removing one of these metal caps and in protecting the other with normal epoxy resin, the contacting wire being sheathed in plastic [37].

Electrochemical experiments were performed with a computer-controlled μ-Autolab type I potentiostat–galvanostat with GPES software (Metrohm-Autolab Ecochemie, Utrecht, The Netherlands).

Electrochemical impedance spectroscopy (EIS) experiments were carried out using a PC-controlled Solartron 1250 Frequency Response Analyzer, coupled to a Solartron 1286 Electrochemical Interface (Solartron Analytical, UK), using ZPlot 2.4 software (Scribner Associates Inc., USA) with an rms perturbation of 10 mV applied over the frequency range 65.5 kHz–0.1 Hz, and 10 frequency values per decade. Impedance spectra were fitted using electrical equivalent circuits with ZView 3.2 software (Scribner Associates Inc., USA).

The pH-measurements were done with a CRISON 2001 micro pH-metre.

The ultrasound bath was a Branson 5210.

All experiments were carried out at room temperature ($25 \pm 1\,^{\circ}C$).

2.3. Modified electrode preparation

In order to have a reproducible surface the CFEs were pretreated in 0.2 M NaCl by cycling the potential 10 times between −1.0 and +1.0 V vs SCE at a scan rate of $100\,mV\,s^{-1}$.

2.3.1. Brilliant green electropolymerisation

The electrodes were treated in 0.1 M sulphuric acid for 10 cycles from −1.0 V up to +1.2 V vs SCE (scan rate $100\,mV\,s^{-1}$) before electropolymerisation.

For electropolymerisation, a 1 mM monomer solution was prepared by dissolving the appropriate quantity of BG in 0.1 M McIlvaine buffer pH 4.0. Then, BG was electropolymerised by cycling the potential (10 cycles) from −1.0 V up to +1.2 V vs SCE with $100\,mV\,s^{-1}$ scan rate.

2.3.2. EDOT electropolymerisation

EDOT was electropolymerised as reported in Ref. [24]. The appropriate amount of monomer was dissolved in 0.1 M NaSS to obtain a concentration of 0.01 M. The solution was then heated and stirred for 30 min until complete dissolution of the monomer, and EDOT was electropolymerised by cycling the potential for 10 times between −0.6 V and +1.2 V vs SCE ($50\,mV\,s^{-1}$).

2.3.3. Carbon nanotubes functionalization

Carbon nanotubes were purified and functionalized by stirring in 5 M nitric acid for one night. The solid was filtered on a filter paper and washed with water until neutral pH. The powder was dried in the oven at 80 °C for one night and collected. This procedure was used to remove metal catalysts and amorphous carbon, derived from the synthesis process, and to functionalize the end of CNTs with —COOH groups.

A solution containing 1% chitosan and 1% acetic acid was prepared and used to form a 1% CNT suspension. After sonication in an ultrasound bath for 3 h, 10 μL were placed on the electrode by drop-casting and left to dry for 1 h, before dropping another 10 μL. Afterwards, electrodes were left to dry in air, for at least 24 h.

2.3.4. Types of electrode

Different architectures were studied in order to understand the role of each compound (PBG, PEDOT, CNT) and to find the best structure for sensing purposes. The carbon resistor electrodes were modified as follows:

- PBG/CFE, PEDOT/CFE, CNT/CFE: each compound was deposited or electropolymerised alone on the CFE, without other modification;
- PEDOT/PBG/CFE and CNT/PBG/CFE: PBG was deposited on the CFE and covered with PEDOT or CNT;
- PBG/PEDOT/CFE and PBG/CNT/CFE: PBG was electropolymerised on the top of the electrode after PEDOT or CNT deposition;
- PEDOT/CNT/CFE and CNT/PEDOT/CFE: electrodes without PBG, for comparison.

All the electrodes were left in air at least for 24 h at ambient temperature before use.

3. Results and discussion

3.1. Electropolymerisation of brilliant green

First, BG, see Fig. 1, was electropolymerised on CFE from a solution containing 1 mM monomer in McIlvaine buffer pH 4.0. The cyclic voltammograms are shown in Fig. 2a and, as observed, at high positive potentials, around 1.0 V, the oxidation currents recorded during the first four cycles, show the formation of cation radicals. From the 4th to the 10th cycle this current begins to decrease, probably because the polymer formed during the first cycles impedes the monomer reaching the electrode surface, no radical cations and little polymer being formed afterwards.

On the contrary, polymerising BG on CNT/CFE, Fig. 2b, gives a continuous increase of the corresponding polymer peaks at around +0.3, +0.5, −0.5 and −0.7 V, indicating that BG is electropolymerised up to the last cycle, since CNTs provide a more open structure for the passage of the monomer, thicker films of PBG being achieved. On PEDOT/CFE, Fig. 2c, polymer formation is demonstrated by the decrease in the capacitive currents of PEDOT with each cycle, due to the entrance of PBG in the structure of PEDOT, which covers the polymer.

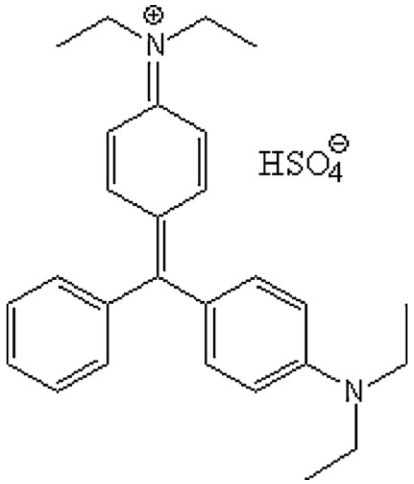

Fig. 1. Chemical structure of brilliant green monomer.

To consider all the possible architectures for the modified electrode, EDOT was also electropolymerised on top of CNT/CFE and

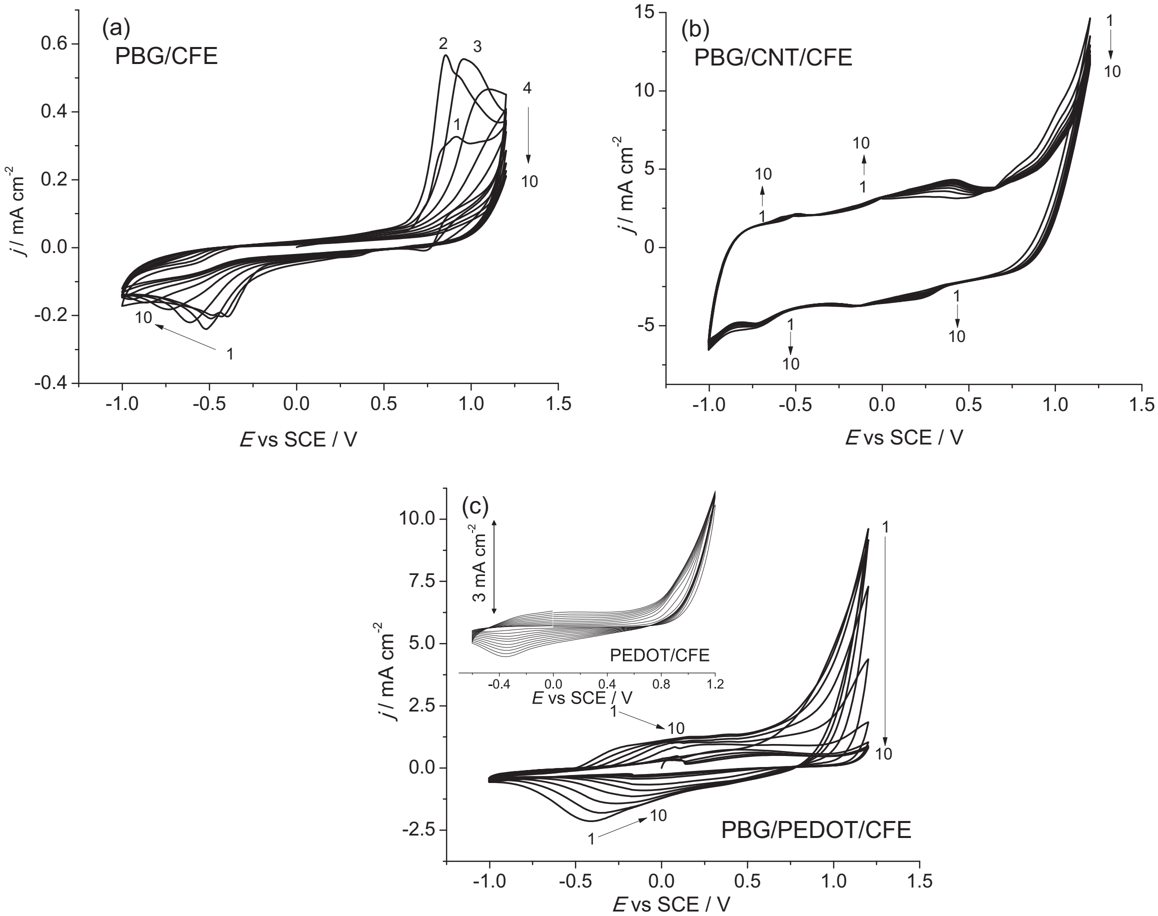

Fig. 2. Electropolymerisation of BG at CFE (a), CNT/CFE (b) and PEDOT/CFE (c) from a solution containing 1 mM monomer in McIlvaine buffer pH 4.0; 10 scans at 100 mV s^{-1}. The inset shows the electropolymerisation of PEDOT at CFE in 0.1 M NaPSS; 10 scans at 50 mV s^{-1}.

PBG/CFE (voltammograms not shown). In the case of CNT, the increase of the capacitive currents corresponding to the formation of the PEDOT film is not so evident as in the case of its deposition on bare CFE (Fig. 2c, inset), because CNTs alone are already very capacitive. When EDOT is electropolymerised on PBG, the profiles of the CVs are very similar to those recorded at the bare electrode, but the current is lower, probably due to a diffusion barrier exhibited by the PBG film.

3.2. *Characterization of the electrodes*

3.2.1. *Cyclic voltammetry*

Cyclic voltammograms were recorded in 0.1 M KCl for all the modified electrodes at scan rates from 10 to 200 mV s^{-1}. They all show a linear dependence of the peak current with the square root of the potential scan rate, so that the electrochemical process at the electrode is controlled by diffusion of the counterion. Moreover, the slope of these linear plots (Table 1) allows a comparison to be made as to how diffusion occurs at different electrodes. For PBG alone, the slope is two and three orders of magnitude lower than for PEDOT and for CNT respectively, demonstrating difficult diffusion through the PBG film. The same was observed for the architectures with PBG on the top of CNT and PEDOT (PBG/CNT and PBG/PEDOT), with slopes lower than for CNT or PEDOT alone. This is probably due to the compact structure of the PBG film.

Comparison of the slope values also allows understanding as to which architecture containing CNT in different positions leads to better diffusion. Indeed, when CNTs are on the top (CNT/PEDOT/CFE and CNT/PBG/CFE) the values of the slope are higher than for CNT covered by polymers (PEDOT/CNT/CFE and PBG/CNT/CFE), since the polymer can fill the porous structure of the CNT, slowing diffusion.

Capacitance values for all the electrodes were calculated and are presented in Table 1. As expected, CNTs considerably increase the capacitance values in all the electrode architectures investigated, including that with PBG, which increases from 0.1 (PBG alone) to 15.4 and 15.7 mF cm^{-2} for PBG/CNT and CNT/PBG, respectively. The presence of PEDOT with CNT, in both positions, PEDOT/CNT/CFE and CNT/PEDOT/CFE, leads to the highest capacitances of 20.5 and 22.8 mF cm^{-2}, respectively, due to the capacitive contribution of both components.

The influence of oxygen was evaluated and no influence for the modified electrodes without PBG was observed, whilst when PBG was present a significant decrease of the current is recorded in the absence of O_2.

Operational stability experiments were undertaken by cycling the potential 100 times from −0.7 V to +0.5 V with the scan rate of 50 mV s^{-1}. The electrodes show a very good stability, since the anodic and cathodic currents of the corresponding peaks of each electrode decrease by only 7% of the initial value after 100 cycles.

3.2.2. *Impedance spectroscopy*

Electrochemical impedance spectroscopy (EIS) was used to study the physical and interface properties of the electrodes. Spectra were recorded in 0.1 M KCl at +0.15, 0.0, −0.2 and −0.4 V vs SCE, values chosen to be in the electroactive regions of the modified electrodes. The complex plane plots are shown in Fig. 3. The electrical circuits used to fit the impedance spectra are presented in Fig. 4 and the values of the equivalent circuit components, obtained from the fitting, are displayed in Table 2.

In the equivalent circuit, R_Ω is the cell resistance, always around 8 Ω cm^2, R_{ct} and R_{pol} represent the charge transfer at the solid-liquid interface and the polarization resistance of the polymer, respectively. CPE_{dl} and CPE_{pol} are constant phase elements representing the charge separation of the double layers and the polarization of the polymer, respectively. $CPE = [(Ci\omega)^\alpha]^{-1}$, modelled as pure capacitor in the case of $\alpha = 1$ or as non-ideal capacitor, due to the porosity and non-homogeneity of the surface, for $0.5 < \alpha < 1$. The diffusional resistance R_W and the diffusional time constant τ are parameters of the open Warburg element, resulting from the equation $Z_W = R_W cth[(\tau i\omega)^\alpha](\tau i\omega)^{-\alpha}$, where $\alpha < 0.5$. C represents the capacitance of the carbon nanotubes.

In the case of PBG/CFE, spectra recorded at +0.15 V, 0.0 V and −0.2 V show a semicircle in the high frequency region with straight lines at low frequencies, while at −0.4 V this line is substituted by a large diameter semicircle. The corresponding electrical equivalent circuit (Fig. 4a) is composed by R_Ω, in series with CPE_{dl} with $\alpha_{dl} = 1$, in parallel with R_{ct}, in series with CPE_{pol}, which has in parallel R_{pol} only at −0.4 V. From +0.15 V to −0.4 V the high-frequency semicircle becomes bigger and, corresponding to an increase of R_{ct}, while the values of CPE_{dl} decrease, since the double layer becomes more resistive and less capacitive at more negative potentials. Note that the values of CPE_{pol} are higher at +0.15 V and −0.4 V, since at these potentials the polymer is electroactive, as shown in the cyclic voltammograms recorded at PBG/CFE.

The spectra of PEDOT/CFE also present a semicircle in the high frequency region, ending with very capacitive straight lines at low frequencies. The impedance values are much lower in this case, indicating a more conductive character of the PEDOT polymer. The equivalent circuit used to fit these spectra is shown in Fig. 4b. From positive to negative potentials, the values of CPE_{dl} decrease and the values of R_{ct} increase, indicating that the polymer is less resistive and more capacitive in the positive potential region. The α_{dl} values close to 0.5 illustrate the high porosity and non-uniformity of the PEDOT/CFE interface. The values of CPE_{pol} are three orders of magnitude higher than that of PBG, and α_{pol} reaches values very close to 1, indicating a pure-like capacitive behaviour of PEDOT polymer.

CNT/CFE show typical capacitive lines with phase angles close to 90° at low frequencies, in agreement with the very high capacitance currents exhibited in the CV experiments. In the high frequency region, spectra present lines with slopes lower than 45°, correlated to diffusional processes through the porous CNT structure. The electrical circuit used for fitting has a Warburg element, R_W, in series with R_Ω for the first part of the spectra in series with a pure

Table 1

Slopes of plots of j_p vs. $\nu^{1/2}$ and capacitance values calculated from the slope of the plot of j vs. ν (cyclic voltammograms recorded in 0.1 M KCl).

Electrode	Anodic slope (μA cm^{-2} mV s^{-1})	Cathodic slope (μA cm^{-2} mV s^{-1})	C (mF cm^{-2})
PBG/CFE	0.03	0.02	0.1
CNT/CFE	21.0	16.1	14.4
PEDOT/CFE	3.0	–	4.2
CNT/PEDOT/CFE	25.0	–	22.8
PEDOT/CNT/CFE	14.1	12.2	20.5
PBG/CNT/CFE	18.2	16.0	15.4
CNT/PBG/CFE	23.3	18.3	15.7
PEDOT/PBG/CFE	4.6	–	2.9
PBG/PEDOT/CFE	2.7	–	4.0

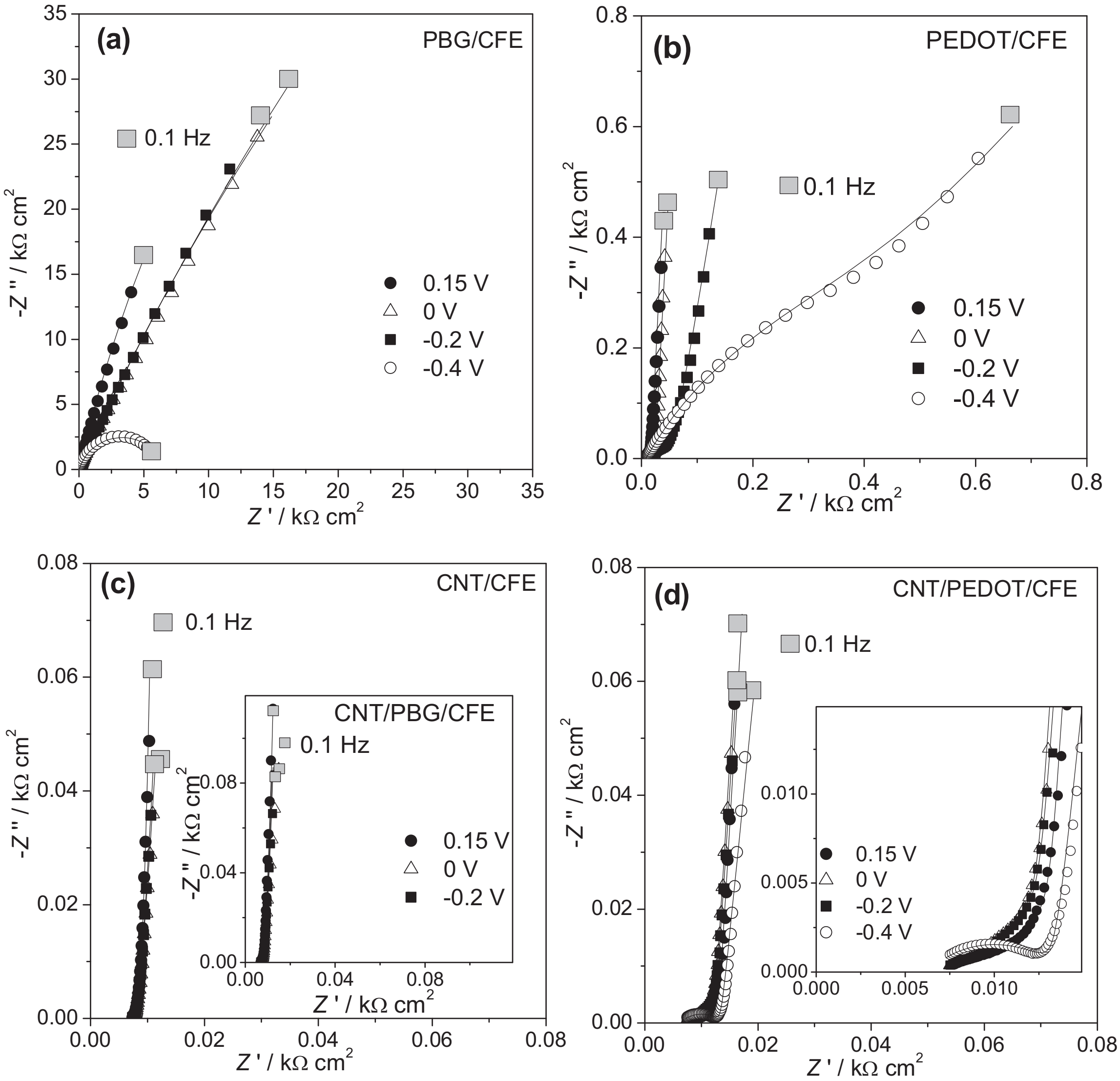

Fig. 3. Complex plane impedance plots recorded in KCl 0.1 M for the electrodes PBG/CFE, PEDOT/CFE, CNT/CFE, CNT/PEDOT/CFE; the lines represent equivalent circuit fitting.

capacitor for the second part (Fig. 4c). At more negative potentials, the diffusional resistance R_W increases, and the capacitance values are in accordance with those obtained from cyclic voltammetry.

In the case of CNT/PBG/CFE and PBG/CNT/CFE the profile of the impedance spectra is very similar to that of CNT/CFE, the same electrical circuit being used for the fitting, with very similar R_W and C values, showing clearly that the overall electrical properties of the electrodes are more influenced by CNTs than by the presence of the redox polymer.

Carbon nanotubes have a dominant influence when together with PEDOT. In particular, PEDOT/CNT/CFE (spectra not shown) presents the same spectral profile as CNT/CFE with insignificant differences in R_W and C values. In the case of CNT/PEDOT/CFE, the diffusional region at high frequency is broader than at CNT/CFE

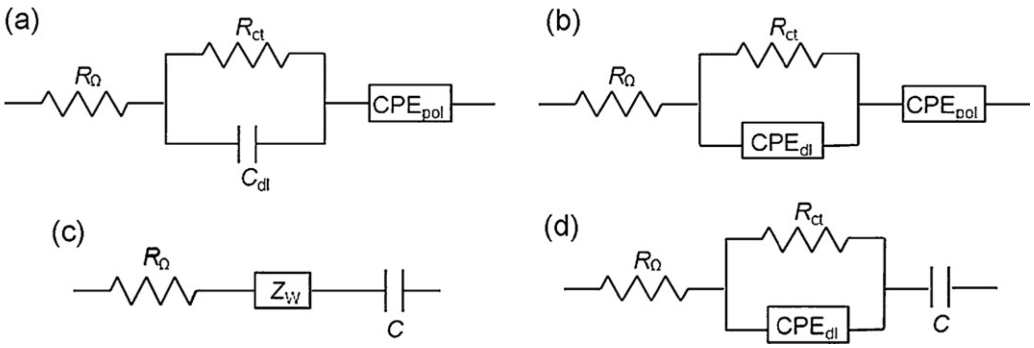

Fig. 4. Equivalents circuits used to fit EIS spectra shown in Fig. 3.

Table 2
Values of the parameters obtained by fitting impedance spectra with the equivalent circuits shown in Fig. 4 for PBG/CFE, PEDOT/CFE, CNT/CFE, CNT/PBG/CFE, CNT/PEDOT/CFE.

Electrode	E_{ap} vs SCE (V)	CPE_{dl} ($mF\,cm^{-2}\,s^{\alpha-1}$)	α_{dl}	R_{ct} ($\Omega\,cm^2$)	CPE_{pol} ($mF\,cm^{-2}\,s^{\alpha-1}$)	α_{pol}	R_{pol} ($\Omega\,cm^2$)	R_W ($\Omega\,cm^2$)	τ (s)	α	C ($mF\,cm^{-2}$)
PBG/CFE	0.15	10.7×10^{-3}	1	2.5	46.9×10^{-3}	0.84	–	–	–	–	–
	0	5.5×10^{-3}	1	2.4	19.3×10^{-3}	0.73	–	–	–	–	–
	−0.2	2.5×10^{-3}	1	6.2	26.7×10^{-3}	0.73	–	–	–	–	–
	−0.4	0.7×10^{-3}	1	10.2	64.7×10^{-3}	0.81	6.7	–	–	–	–
PEDOT/CFE	0.15	3.1	0.51	10.1	3.6	0.97	–	–	–	–	–
	0	3.5	0.50	18.0	3.4	0.97	–	–	–	–	–
	−0.2	1.9	0.55	53.4	3.0	0.90	–	–	–	–	–
	−0.4	0.7	0.74	313.6	1.3	0.60	–	–	–	–	–
CNT/CFE	0.15	–	–	–	–	–	–	0.4	0.003	0.19	13.2
	0	–	–	–	–	–	–	1.8	0.094	0.37	21.1
	−0.2	–	–	–	–	–	–	2.0	0.136	0.34	20.0
CNT/PBG/CFE	0.15	–	–	–	–	–	–	0.9	0.016	0.19	14.2
	0	–	–	–	–	–	–	1.1	0.024	0.19	18.9
	−0.2	–	–	–	–	–	–	1.0	0.022	0.19	19.5
CNT/PEDOT/CFE	0.15	–	–	–	–	–	–	5.1	0.119	0.13	24.0
	0	–	–	–	–	–	–	4.0	0.080	0.16	29.9
	−0.2	–	–	–	–	–	–	4.4	0.113	0.16	30.7
	−0.4	1.8	0.52	7.8	–	–	–	–	–	–	25.5

alone and at the most negative potential used (−0.4 V) the diffusional line becomes a very depressed semicircle (electrical circuit shown in Fig. 4d). Moreover, the values of the resistance increase from +0.15 V to −0.4 V and are higher than those of CNT/CFE and PEDOT/CNT/CFE. All these changes can be explained considering that CNTs deposited in the porous structure of PEDOT are more disordered than when deposited on bare electrodes, and hence cause a more chaotic and difficult diffusion. On the contrary, polymerisation of EDOT on the CNTs gives the electrode a more ordered architecture (data not shown). However, CNT/PEDOT/CFE shows the highest capacitance values, between 24 and 31 mF cm^{-2}, higher than CNT/CFE (13–21 mF cm^{-2}) and PEDOT/CNT/CFE (data not shown), in agreement with the cyclic voltammetry results.

Impedance was also performed at PEDOT/PBG/CFE and PBG/PEDOT/CFE for comparison. The profile of the spectra and also the equivalent circuit (Fig. 4b) remain the same as for PEDOT/CFE, showing that PEDOT has the main influence on the electrode characteristics. However, R_{ct} is higher and CPE_{dl}, α_{dl} and CPE_{pol} lower than PEDOT/CFE, demonstrating that the combinations PEDOT and PBG are worse than PEDOT alone for application in electroanalysis.

Oxygen can influence the behaviour of the electrodes because it can oxidize the conducting polymer and can be reduced at the interface, thus affecting the homogeneity of the film. For these reasons impedance spectra were also registered in the absence of oxygen, removed from the solution by bubbling N_2 for at least 20 min. Some influence of oxygen can be seen in the changes of equivalent circuit component values.

For PBG/CFE, the absence of O_2 leads to an increase in the R_{ct} values, and CPE_{pol} decreases only at +0.15 V and −0.4 V, where the polymer is electroactive. Probably, the redox activity of the polymer involves oxygen or is favoured by it. Oxygen has a lesser influence on PEDOT/CFE. In this case R_{ct} increases probably because fewer hydroxyl ions are formed, which may help the electron transfer at the surface of the electrode substrate. More importantly, the electrodes containing CNTs in their architecture are not influenced at all by oxygen, showing again advantages in using the CNTs for the construction of (bio)sensors.

3.3. Hydrogen peroxide determination

The characterization of the electrodes showed that each type of compound used to modify the bare electrode can greatly influence the general properties. To further investigate which type of electrode architecture is better for electroanalytical purposes, a study of the modified electrodes' behaviour towards hydrogen peroxide determination was performed.

Hydrogen peroxide [38] was chosen as analyte because it is a simple compound, but with great importance in pharmaceutical, clinical, environmental, mining, textile and food manufacturing applications. H_2O_2 is also a side product generated from some classic biochemical reactions catalysed by many oxidase enzymes. For these reasons, H_2O_2 appears to be the best species to evaluate the possible application of the modified electrodes as sensors and biosensors.

Preliminary analysis was performed by potential cycling between −0.7 V and +0.7 V for each electrode in 0.1 M NaPBS (pH = 7) as electrolyte, in the absence and presence of H_2O_2. The cyclic voltammograms (not shown) for the electrodes without carbon nanotubes (PBG/CFE, PEDOT/CFE, PEDOT/PBG/CFE and PBG/PEDOT/CFE) do not exhibit a significant response towards H_2O_2. On the contrary, CNT-based electrodes show the electroreduction of H_2O_2 at a potential around −0.1 V (Fig. 5a). These results together with impedance and voltammetric studies, lead to the exclusion of the electrodes without CNTs from further applications.

Chronoamperometry at fixed potential was performed in the same electrolyte solution at 0.0 V vs SCE for all the electrodes based

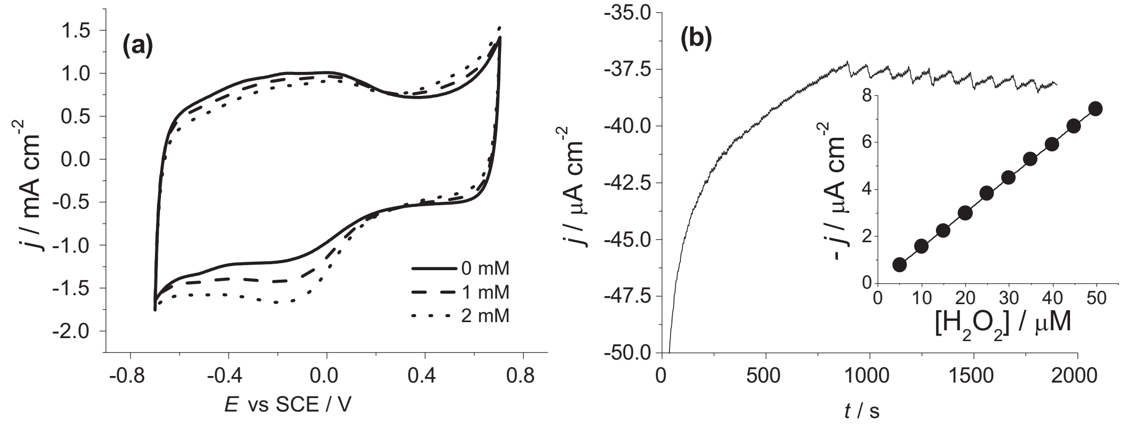

Fig. 5. (a) Cyclic voltammograms recorded in a solution containing NaPBS 0.1 M before and after addition of H_2O_2 and (b) Amperometric response to H_2O_2 at CNT/PBG/CFE with the corresponding calibration plot shown in the inset.

on CNTs. More negative potentials were also applied, and indeed higher sensitivities were achieved, but 0.0 V was chosen since the electrodes still exhibited a good response to hydrogen peroxide, and also because it has the important advantage to avoid possible interferences. A typical chronoamperometric response in the concentration range between 5 to 50 μM H_2O_2 is shown in Fig. 5b with the corresponding calibration plot in inset.

PEDOT/CNT/CFE and PBG/CNT/CFE, show smaller sensitivities of 91.4 ± 0.4 and 113.5 ± 0.6 μA cm^{-2} mM^{-1} and higher detection limits of 2.40 and 1.45 μM than CNT/CFE (124.5 ± 0.4 μA cm^{-2} mM^{-1}, 1.19 μM), indicating that the coverage of CNTs with a polymer reduces their activity, probably because the surface area and the number of active sites decrease. On the other hand, when CNTs are placed on the top of the polymer modified electrode, the sensitivity is higher and detection limits are smaller, an improvement compared to CNTs alone. In the case of CNT/PEDOT/CFE, the improvement in sensitivity to 131.9 ± 0.5 μA cm^{-2} mM^{-1} and in the detection limit to 0.89 μM is already expected considering the high capacitance values obtained from CV and EIS results. In the case of CNT/PBG/CFE, even if PBG do not contribute to the total capacitance of the electrode, the detection limit is comparable with CNT/PEDOT/CFE (0.91 μM) and the best sensitivity of 151.8 ± 0.6 μA cm^{-2} mM^{-1} is obtained, indicating that PBG improves H_2O_2 detection.

Repeatability was verified constructing three new electrodes of each type and testing them in the same conditions. Fig. 6 shows calibration plots in the low concentration range for CNT/PEDOT/CFE and CNT/PBG/CFE. The points are obtained from the mean of the values for the three electrodes and the error bars represent the standard deviations for each point. Repeatability results were excellent, RSD values being lower than 1%.

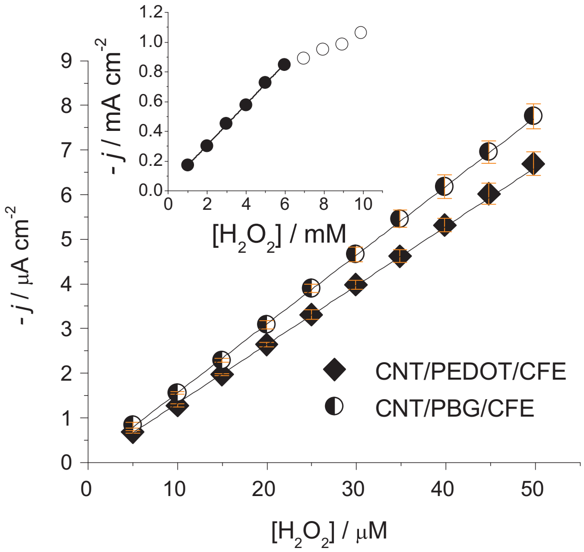

Fig. 6. Linear calibration plots corresponding to CNT/PBG/CFE and CNT/PEDOT/CFE in NaPBS 0.1 M at 0.0 V obtained in the concentration range from 5 to 50 μM H_2O_2. Inset: typical calibration plot obtained for high concentration range.

The inset of Fig. 6 presents an example of a calibration plot for higher concentrations of H_2O_2. All the electrode types have very similar sensitivities, reaching saturation at 6 mM H_2O_2.

Stability was evaluated recording a 7-point calibration plot in the concentration range of 5–50 μM for H_2O_2, three times a week.

Table 3
Performance parameters of hydrogen peroxide sensors for different modified electrodes recently reported in the literature.

Electrode	Concentration range (mM)	S (μA cm^{-2} mM^{-1})	LOD (μM)	Potential (V)	Ref.
MnO_2/VACNTs	0.001–1.8	1001.0	0.80	+0.45	[39]
SiNW/AgNPs	0.2–70	57.5	0.20	−0.45	[40]
HRP/PAM/MWCNTCOOH/Au	0.086–10	194.9	26.0	−0.35	[41]
HRP/AuNPs/BC	0.0003–1.00	610.0	0.10	+0.15	[42]
HRP/Sulf-G	0.003–0.33	557.0	1.17	−0.35	[43]
HRP/3DAuNW	0.1–15	45.9	0.42	−0.1	[44]
Graphene/PB	0.1–15.5	408.7	0.34	+0.1	[45]
N-CNTs	0.002–0.14	24.5	0.37	+0.3	[46]
PB/MWCNT	0.001–5	856.0	0.02	+0.1	[47]
PAA-BO/Au	0.025–2.5	311.2	5.00	−0.5	[48]
Ag-UTPNSs	0.1–90	4.5	0.57	−0.35	[49]
PPy/magnetite hybrid	0–0.4	72.0	–	−0.3	[50]
CNT/PBG/CFE	0.0005–6	151.8	0.91	0.0	This work

After 20 days the sensitivity decreases by only 10% from its initial value, after this period decreasing very fast.

In Table 3, comparison with recent (2010–2012) literature data of modified electrodes for hydrogen peroxide sensing is presented. The values of operation ranges and sensitivities are comparable with the other types of sensors and the detection limit is very similar, but this new electrode has the advantage to work at 0.0 V unlike the others, allowing the avoidance of the majority of interferences.

4. Conclusions

Brilliant green, belonging to the family of triphenylmethane dyes, has been successfully electropolymerised on non-modified (CFE) and for the first time on modified (PEDOT or CNT) electrodes. The polymerisation occurs during the first four cycles and allows the formation of a very compact polymer film on the electrode. The presence of a closed PBG structure is confirmed by CV studies that show lower diffusion coefficients and capacitances for the electrodes with PBG. On the contrary, when CNTs are on the top of the electrode (CNT/PEDOT/CFE and CNT/PBG/CFE) the diffusion is facilitated. Both CNT and PEDOT increase the capacitance values of the electrodes, the highest value being recorded at CNT/PEDOT/CFE. EIS confirms the CV results, showing additionally that PBG-based electrodes are influenced by dissolved oxygen, while the CNT containing ones are not.

Application to H_2O_2 detection was achieved with better sensitivities when CNTs are placed on the top of PEDOT and PBG modified electrodes, showing an improvement compared to CNTs alone, the highest sensitivity being recorded at CNT/PBG/CFE, indicating that PBG improves the H_2O_2 detection. Reproducibility studies at CNT/PBG and CNT/PEDOT/CFE were excellent with RSD lower than 1% and together with the good stability of the newly developed electrodes show their excellent applicability for the development of improved electrochemical sensors and biosensors.

Acknowledgments

Valentina Pifferi thanks the LLP Erasmus Placement for a grant. Financial support from Fundação para a Ciência e a Tecnologia (FCT), Portugal, PTDC/QUI-QUI/116091/2009, POCH, POFC-QREN (co-financed by FSE and European Community Fund FEDER/COMPETE) and FCT project PEst-C/EME/UI0285/2011 (CEMUC® – Research Unit 285), Portugal, is gratefully acknowledged. MMB and MEG thank FCT for postdoctoral grants SFRH/BPD/72656/2010 and SFRH/BPD/36930/2007, respectively.

References

[1] M. Gerard, A. Chaubey, B.D. Malhotra, Application of conducting polymers to biosensors, Biosensors and Bioelectronics 17 (2002) 345.
[2] Rajesh, T. Ahuja, D. Kumar, Recent progress in the development of nano-structured conducting polymers/nanocomposites for sensor applications, Sensors and Actuators B 136 (2009) 275.
[3] C. Li, H. Bai, G. Shi, Conducting polymer nanomaterials: electrosynthesis and applications, Chemical Society Reviews 38 (2009) 2397.
[4] G. Inzelt, M. Pineri, J.W. Schultze, M.A. Vorotyntsev, Electron and proton conducting polymers: recent developments and prospects, Electrochimica Acta 45 (2000) 2403.
[5] M.E. Ghica, C.M.A. Brett, Development of a novel glucose and pyruvate biosensors at poly(neutral red) modified carbon film electrodes. Application to natural samples, Electroanalysis 18 (8) (2006) 748.
[6] M.M. Barsan, E.M. Pinto, C.M.A. Brett, Electrosynthesis and electrochemical characterisation of phenazine polymers for application in biosensors, Electrochimica Acta 53 (2008) 3973.
[7] M.E. Ghica, C.M.A. Brett, Poly(brilliant cresyl blue) modified glassy carbon electrodes: electrosynthesis, characterisation and application in biosensors, Journal of Electroanalytical Chemistry 629 (2009) 35.
[8] A.A. Karyakin, E.E. Karyakina, H.-L. Schmidt, Electropolymerized azines: a new group of electroactive polymers, Electroanalysis 11 (1999) 149.
[9] R. Pauliukaite, M.E. Ghica, M.M. Barsan, C.M.A. Brett, Phenazines and polyphenazines in electrochemical sensors and biosensors, Analytical Letters 43 (2010) 1588.
[10] R. Pauliukaite, C.M.A. Brett, Poly(neutral red): electrosynthesis, characterisation and application as a redox mediator, Electroanalysis 12 (2008) 1275.
[11] X. Hu, K. Jiao, W. Sun, J.-Y. You, Electrochemical and spectroscopic studies on the interaction of malachite green with DNA and its application, Electroanalysis 18 (6) (2006) 613.
[12] H. Yi, W. Qu, W. Huang, Electrochemical determination of malachite green using a multi-wall carbon nanotube modified glassy carbon electrode, Mikrochimica Acta 160 (2008) 291.
[13] Q. Wan, X. Wang, X. Wang, N. Yang, Poly(malachite green) film: electrosynthesis, characterization, and sensor application, Polymer 47 (2006) 7684.
[14] X. Wang, N. Yang, Q. Wan, X. Wang, Catalytic capability of poly(malachite green) films based electrochemical sensor for oxidation of dopamine, Sensors and Actuators B 128 (2007) 83.
[15] S.-M. Chen, J.-Y. Chen, R. Thangamuthu, Electrochemical preparation of poly(malachite green) film modified Nafion-coated glassy carbon electrode and its electrocatalytic behavior towards NADH, dopamine and ascorbic acid, Electroanalysis 19 (2007) 1531.
[16] M.E. Ghica, Y. Wintersteller, C.M.A. Brett, Poly(brilliant green)/carbon nanotube modified carbon film electrodes and application as sensors, Journal of Solid State Electrochemistry (2013), http://dx.doi.org/10.1007/s10008-013-2040-4.
[17] B.K. Nandi, A. Goswami, M.K. Purkait, Adsorption characteristics of brilliant green dye on kaolin, Journal of Hazardous Materials 161 (2009) 387.
[18] A. Mittal, D. Kaur, J. Mittal, Applicability of waste materials – bottom ash and deoiled soya – as adsorbents for the removal and recovery of a hazardous dye, brilliant green, Journal of Colloid and Interface Science 326 (2008) 8.
[19] D.W. Breiby, E.J. Samuelsen, L.B. Groenendaal, B. Struth, Smectic structures in electrochemically prepared poly(3,4-ethylenedioxythiophene) films, Journal of Polymer Science Part B: Polymer Physics 41 (2003) 945.
[20] X. Crispin, F.L.E. Jakobsson, A. Crispin, P.C.M. Grim, P. Andersson, A. Volodin, C. Van Haesendonck, M. Van der Auweraer, W.R. Salaneck, M. Berggren, The origin of the high conductivity of poly(3,4-ethylenedioxythiophene)-poly(styrenesulfonate) (PEDOT-PSS) plastic electrodes, Chemistry of Materials 18 (2006) 4354.
[21] J.C. Carlberg, O. Inganas, Poly(3,4-ethylenedioxythiophene) as electrode material in electrochemical capacitors, Journal of the Electrochemical Society 144 (1997) L61.
[22] L. Zhang, X. Duan, Y. Wen, J. Xu, Y. Yao, Y. Lu, L. Lu, O. Zhang, Electrochemical behaviors of roxithromycin at poly(3,4-ethylenedioxythiophene) modified gold electrode and its electrochemical determination, Electrochimica Acta 72 (2012) 179.
[23] L. Pigani, A. Culetu, A. Ulrici, G. Foca, M. Vignali, R. Seeber, PEDOT modified electrodes in amperometric sensing for analysis of red wine samples, Food Chemistry 129 (2011) 226.
[24] S. Kakhki, M.M. Barsan, E. Shams, C.M.A. Brett, Development and characterization of poly(3,4-ethylenedioxythiophene)-coated poly(methylene blue)-modified carbon electrodes, Synthetic Metals 161 (2012) 2718.
[25] A.R. Gonçalves, M.E. Ghica, C.M.A. Brett, Preparation and characterisation of poly(3,4-ethylenedioxythiophene) and poly(3,4-ethylenedioxythiophene)/poly(neutral red) modified carbon film electrodes, and application as sensors for hydrogen peroxide, Electrochimica Acta 56 (2011) 3685.
[26] S. Thiagarajau, M. Rajkumar, S.-M. Chen, Nano TiO_2–PEDOT film for the simultaneous detection of ascorbic acid and diclofenac, International Journal of Electrochemical Science 7 (2012) 2109.
[27] N.F. Atta, A. Galal, E.H. El-Ads, Gold nanoparticles-coated poly(3,4-ethylenedioxythiophene) for the selective determination of sub-nano concentrations of dopamine in presence of sodium dodecyl sulfate, Electrochimica Acta 69 (2012) 102.
[28] C.N.R. Rao, B.C. Satishkumar, A. Govindaraj, M. Nath, Nanotubes, ChemPhysChem 2 (2001) 78.
[29] J.J. Gooding, Nanostructuring electrodes with carbon nanotubes: a review on electrochemistry and applications for sensing, Electrochimica Acta 50 (2005) 3049.
[30] G. Lota, K. Fic, E. Frackowiak, Carbon nanotubes and their composites in electrochemical applications, Energy and Environmental Science 4 (2011) 1592.
[31] M. Valcárcel, B.M. Simonet, S. Cárdenas, B. Suárez, Present future applications of carbon nanotubes to analytical science, Analytical and Bioanalytical Chemistry 382 (2005) 1783.
[32] R.C. Peña, M. Bertotti, C.M.A. Brett, Methylene blue/multiwall carbon nanotube modified electrode for the amperometric determination of hydrogen peroxide, Electroanalysis 23 (10) (2011) 2290.
[33] M.E. Ghica, C.M.A. Brett, The influence of carbon nanotubes and polyazine redox mediators on the performance of amperometric enzyme biosensors, Mikrochimica Acta 170 (2010) 257.
[34] J.-Y. Chin, C.-M. Yu, M.-J. Yen, L.-C. Chen, Glucose sensing electrodes based on a poly(3,4-ethylenedioxythiophene)/Prussian blue bilayer and multi-walled carbon nanotubes, Biosensors and Bioelectronics 24 (2009) 2015.
[35] P. AbiramaSundari, P. Manisankar, Development of ultrasensitive surfactants doped poly(3,4-ethylenedioxythiophene)/multiwalled carbon nanotube sensor for the detection of pyrethroids and an organochlorine pesticide, Journal of Applied Electrochemistry 41 (2011) 29.

[36] Y. Umasankara, A.P. Periasamy, S.-M. Chen, Electrocatalysis and simultaneous determination of catechol and quinol by poly(malachite green) coated multiwalled carbon nanotube film, Analytical Biochemistry 411 (2011) 71.

[37] O.M.S. Filipe, C.M.A. Brett, Characterization of carbon film electrodes for electroanalysis by electrochemical impedance, Electroanalysis 16 (2004) 994.

[38] W. Chen, S. Cai, Q.-Q. Ren, W. Wen, Y.-D. Zhao, Recent advances in electrochemical sensing for hydrogen peroxide: a review, Analyst 137 (2012) 49.

[39] B. Xu, M.-L. Ye, Y.-X. Yu, W.-D. Zhang, A highly sensitive hydrogen peroxide amperometric sensor based on MnO_2-modified vertically aligned multiwalled carbon nanotubes, Analytica Chimica Acta 674 (2010) 20.

[40] J. Yin, X. Qi, L. Yang, G. Hao, J. Li, J. Zhong, A hydrogen peroxide electrochemical sensor based on silver nanoparticles decorated silicon nanowire arrays, Electrochimica Acta 56 (2011) 3884.

[41] M.-Y. Hua, Y.-C. Lin, R.-Y. Tsai, H.-C. Chen, Y.-C. Liu, A hydrogen peroxide sensor based on a horseradish peroxidase/polyaniline/carboxy-functionalized multiwalled carbon nanotube modified gold electrode, Electrochimica Acta 56 (2011) 9488.

[42] W. Wang, T.-J. Zhang, D.-W. Zhang, H.-Y. Li, Y.-R. Ma, L.-M. Qi, Y.-L. Zhou, X.-X. Zhang, Amperometric hydrogen peroxide biosensor based on the immobilization of heme proteins on gold nanoparticles–bacteria cellulose nanofibers nanocomposite, Talanta 84 (2011) 71.

[43] Q. Zhang, Y. Qiao, L. Zhang, S. Wu, H. Zhou, J. Xu, X.-M. Song, Direct electrochemistry and electrocatalysis of horseradish peroxidase immobilized on water soluble sulfonated graphene film via self-assembly, Electroanalysis 23 (2011) 900.

[44] J. Xu, F. Shang, J.H.T. Luong, K.M. Razeeb, J.D. Glennon, Direct electrochemistry of horseradish peroxidase immobilized on a monolayer modified nanowire array electrode, Biosensors and Bioelectronics 25 (2010) 1313.

[45] Y. Zhang, X. Sun, L. Zhu, H. Shen, N. Jia, Electrochemical sensing based on graphene oxide/Prussian blue hybrid film modified electrode, Electrochimica Acta 56 (2011) 1239.

[46] X. Xu, S. Jiang, Z. Hu, S. Liu, Nitrogen-doped carbon nanotubes: high electrocatalytic activity toward the oxidation of hydrogen peroxide and its application for biosensing, ACS Nano 4 (2010) 4292.

[47] D. Du, M. Wang, Y. Qin, Y. Lin, One-step electrochemical deposition of Prussian blue-multiwalled carbon nanotube nanocomposite thin-film: preparation, characterization and evaluation for H_2O_2 sensing, Journal of Materials Chemistry 20 (2010) 1532.

[48] M.-Y. Hua, H.-C. Chen, C.-K. Chuang, R.-Y. Tsai, J.-L. Jeng, H.-W. Yang, Y.-T. Chern, The intrinsic redox reactions of polyamic acid derivatives and their application in hydrogen peroxide sensor, Biomaterials 32 (2011) 4885.

[49] M.R. Mahmoudiana, Y. Alias, W.J. Basirun, M. Ebadi, Preparation of ultrathin polypyrrole nanosheets decorated with Ag nanoparticles and their application in hydrogen peroxide detection, Electrochimica Acta 72 (2012) 46.

[50] G. Bencsik, C. Janáky, B. Endrodi, C. Visy, Electrocatalytic properties of the polypyrrole/magnetite hybrid modified electrode towards the reduction of hydrogen peroxide in the presence of dissolved oxygen, Electrochimica Acta 73 (2012) 53.